Journal of Alloys and Compounds, 190 (1993) 229–235
JALCOM 441

Crystal and magnetic structures of the permanent magnet material $R_2Fe_{14}C_{0.95}B_{0.05}$ (R ≡ Ce, Pr)

Ch. Hellwig and K. Girgis
Institut für Kristallographie und Petrographie, ETHZ, CH-8092 Zürich (Switzerland)

K. H. J. Buschow
Philips Research Laboratories, 5600 JA Eindhoven (Netherlands)

P. Fischer and J. Schefer
Labor für Neutronenstreuung, ETHZ–PSI, CH-5232 Villigen PSI (Switzerland)

(Received 19 July, 1992)

Abstract

Investigations of the compounds $R_2Fe_{14}C_{0.95}B_{0.05}$ (R ≡ Ce, Pr) by means of X-ray and neutron diffraction as well as by metallographic techniques and differential thermal analysis (DTA) were carried out. Both compounds crystallize in the tetragonal space group $P4_2/mnm$ and are isotypic to $Nd_2Fe_{14}B$. Lattice constants at 295 K are $a = 8.7579(3)$ Å, $c = 11.8867(8)$ Å, for $Ce_2Fe_{14}C_{0.95}B_{0.05}$ and $a = 8.8138(5)$ Å, $c = 12.0541(15)$ Å for $Pr_2Fe_{14}C_{0.05}B_{0.05}$. The samples contained no additional phases except for metallic iron because of the small amount of boron. The nuclear and magnetic structures of the two compounds were investigated by means of neutron diffraction at 643 K (above the Curie temperature T_c), at room temperature and below 25 K. For $Ce_2Fe_{14}C_{0.95}B_{0.05}$ an additional measurement at 423 K was carried out. The magnetic moments of the iron atoms are oriented parallel to the c axis for both compounds. Only small magnetic moments of the rare earth atoms were observed at 12 K for the cerium compound. For the praseodymium compound the magnetic moments of the praseodymium atoms lie parallel to those of the iron atoms. DTA measurements yield a T_c value of 347 K for the cerium compound and 520 K for the praseodymium compound. A pronounced change in the specific heat capacity was measured at 515 K for the cerium compound.

1. Introduction

Since the promising group of permanent magnet materials $R_2Fe_{14}B$ (R is a rare earth metal) was discovered in 1984 [1], many investigations of such new ternary compounds have taken place. Magnetic and structural properties of these compounds are reviewed in ref. 2. Another promising group of permanent magnet materials is that of the isotypic compounds $R_2Fe_{14}C$ [3–7], although their Curie temperatures are slightly lower than those of the corresponding $R_2Fe_{14}B$ systems (*e.g.* 535 K for $Nd_2Fe_{14}C$ [8], compared with 585 K for $Nd_2Fe_{14}B$ [2]). However, the $R_2Fe_{14}C$ compounds have the advantage of the presence of a solid state transformation at high temperatures which can be used to obtain high coercivity bulk material without the necessity of employing the powder metallurgical route [2]. Indeed, the transformation temperatures for the light rare earth compounds are too low to achieve this phase by annealing [9]. To stabilize the tetragonal phase at higher temperatures a small amount of boron was used. Several heavy rare earth compounds $R_2Fe_{14}C$ (R ≡ Tb, Ho, Tm, Lu) have already been studied [10–13]. In another recent independent publication [14] the magnetic structures of $R_2Fe_{14}C$ (R ≡ Lu, Er, Dy) were also determined by neutron diffraction. The aim of the present work is to study the magnetic structure of light rare earth compounds with small additions of boron and to understand the magnetic behaviour of the $R_2Fe_{14}C$ group.

2. Experimental details

The $R_2Fe_{14}C_{0.95}B_{0.05}$ compounds were prepared by arc melting from starting materials of at least 99.9% purity. Afterwards the sample was wrapped in tantalum foil and sealed in an evacuated quartz tube. Vacuum annealing was performed subsequently for 5 weeks at 800 °C. The microstructure of the annealed sample was studied by standard metallographic techniques. The microhardness measurements were carried out to prove homogeneity.

0925-8388/93/$6.00

X-ray powder photographs were obtained using a Guinier focusing camera (Jagodzinski type) with silicon as an internal standard. The intensities were measured by means of an automatic Guinier film scanner. Differential thermal analysis (DTA) was carried out at a heating rate of 10 °C min^{-1}.

The neutron diffraction measurements were carried out for $Ce_2Fe_{14}C_{0.95}B_{0.05}$ at 643 K, at 423 K, at room temperature (295 K) and at 12 K and for $Pr_2Fe_{14}C_{0.95}B_{0.05}$ at 643 K, at room temperature (295 K) and at 23 K. The measurements were performed on the multidetector powder diffractometer DMC [15], using the high resolution mode, at the 10 MW reactor SAPHIR (PSI) with neutrons of wavelength $\lambda = 1.699(2)$, 1.701(2) and 1.703(2) Å.

3. Results

3.1. Metallographic, differential thermal analysis and X-ray results

Figures 1 and 2 show micrographs of the samples. Bright grains arranged in lines are visible in the matrix of $R_2Fe_{14}C_{0.95}B_{0.05}$. These grains are supposed to be free iron (*ca.* 3–4 vol.%). The dark areas are due to pores and oxides. The microhardness measurements show that both samples are homogeneous. The average value of 10 microhardness measurements in the $R_2Fe_{14}C_{0.95}B_{0.05}$ matrix amounts to 688(16) HV for the cerium compound and 686(57) HV for the praseodymium compound.

DTA measurements yield at T_c value of 347 K for the cerium compound and a T_c value of 520 K for the praseodymium compound, while bulk magnetization measurements yield a T_c value of 345 K for the cerium compound and a T_c value of 520 K for the praseodymium compound. By means of DTA a pronounced change in the specific heat capacity was measured at 515 K for the cerium compound.

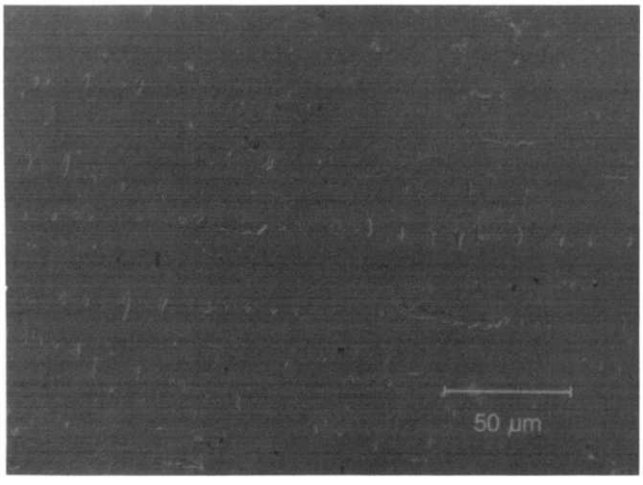

Fig. 1. Micrograph of the $Ce_2Fe_{14}C_{0.95}B_{0.05}$ sample. The sample was polished with diamond particles (less than 1 µm) and subsequently etched in an ethanol–acetic acid solution. Bright grains of free iron are visible in the matrix of $Ce_2Fe_{14}C_{0.95}B_{0.05}$.

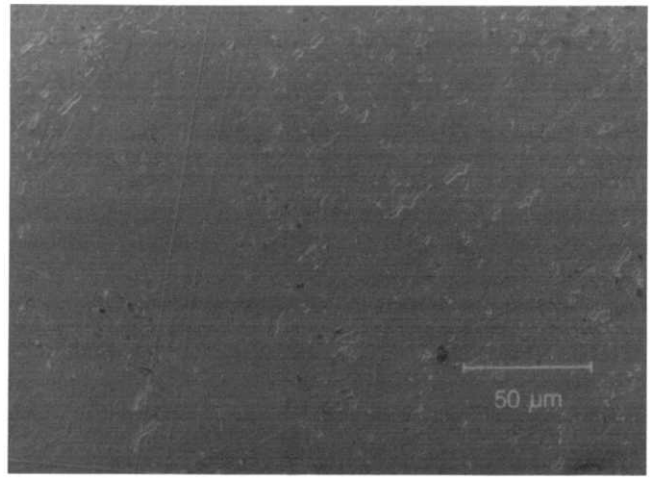

Fig. 2. Micrograph of the $Pr_2Fe_{14}C_{0.95}B_{0.05}$ sample. The sample was polished with diamond particles (less than 1 µm) and subsequently etched in an ethanol–acetic acid solution. Bright grains of free iron are visible in the matrix of $Pr_2Fe_{14}C_{0.95}B_{0.05}$.

The X-ray data show that both compounds crystallize in the tetragonal space group $P4_2/mnm$ (no. 136) with 68 atoms per unit cell and that both samples contain also a certain amount of metallic iron. X-ray powder photographs at room temperature yield lattice constants $a = 8.7579(3)$ Å, $c = 11.8867(8)$ Å, for $Ce_2Fe_{14}C_{0.95}B_{0.05}$ and $a = 8.8138(5)$ Å, $c = 12.0541(15)$ Å, for $Pr_2Fe_{14}C_{0.95}B_{0.05}$.

3.2. Nuclear and magnetic structures

We used as starting parameters those published in ref. 10 for $Tb_2Fe_{14}C$. The rare earth atoms are distributed over two point positions, whereas the iron atoms are distributed over six point positions; the metalloids occupy one further point position. In order to avoid the influence of magnetic intensities on the structure refinement, we studied both compounds at 643 K in the paramagnetic state. The measurements at room temperature and below 25 K yield information concerning magnetic saturation. The scattering lengths used for refinement are 0.484×10^{-12} cm for cerium, 0.458×10^{-12} cm for praseodymium, 0.954×10^{-12} cm for iron and 0.665×10^{-12} cm for boron and for carbon [16, 17]. Therefore the metalloids cannot be distinguished. The neutron magnetic form factors were taken from Freeman and Desclaux [18] (Ce^{3+}, Pr^{3+}) and from Moon [19] (iron). The magnetic form factor curve of Pr^{3+} was calculated using the mean values of j_0 and j_2 of Ce^{3+} and Nd^{3+}.

A two-phase Rietveld refinement [20, 21] was carried out because of the presence of traces of free iron. The

orientation of the magnetic moments is always parallel to the c axis as this delivers significantly better refinements. At 295 K the magnetic moments of the cerium atoms are set to zero as this delivers a slight improvement in the refinement, whereas at 12 K a refinement of these moments was successful ($R_{magnetic}$ slightly better for antiparallel coupling of magnetic iron and cerium moments). The results of the structure refinements are summarized in Tables 1–8, and four patterns are shown in Figs. 3–6. For comparison the magnetic moments achieved by a refinement of $Ce_2Fe_{14}C_{0.95}B_{0.05}$ with the cerium moment set to zero at 12 K are listed in Table 5.

TABLE 1. Structural parameters of $Ce_2Fe_{14}C_{0.95}B_{0.05}$ at 643 K

Atom	Position	Parameter		
		x	y	z
Ce(1)	4f	0.2623(8)	0.2623(8)	0.000
Ce(2)	4g	0.1408(9)	0.8592(9)	0.000
Fe(1)	$16k_1$	0.2247(3)	0.5657(3)	0.1216(2)
Fe(2)	$16k_2$	0.0362(3)	0.3585(3)	0.1775(2)
Fe(3)	$8j_1$	0.0983(3)	0.0983(3)	0.2059(3)
Fe(4)	$8j_2$	0.3172(3)	0.3172(3)	0.2444(3)
Fe(5)	4e	0.000	0.000	0.6078(5)
Fe(6)	4c	0.000	0.500	0.000
C,B	4g	0.3710(7)	0.6290(7)	0.000

$B_{Ce} = 1.16(12)$ Å^2, $B_{Fe} = 0.94(2)$ Å^2, $B_{C,B} = 1.99(16)$ Å^2
$a,b = 8.7672(2)$ Å, $c = 11.8956(4)$ Å
$R_{nuclear} = 3.6\%$, $R_{profile} = 6.3\%$, $R_{expected} = 3.9\%$

The standard deviations of the lattice constants do not include errors $\Delta\lambda/\lambda$ from the neutron wavelength.

TABLE 2. Structural parameters of $Ce_2Fe_{14}C_{0.95}B_{0.05}$ at 423 K

Atom	Position	Parameter		
		x	y	z
Ce(1)	4f	0.2622(8)	0.2622(8)	0.000
Ce(2)	4g	0.1444(9)	0.8556(9)	0.000
Fe(1)	$16k_1$	0.2244(3)	0.5657(3)	0.1217(2)
Fe(2)	$16k_2$	0.0356(3)	0.3587(3)	0.1774(2)
Fe(3)	$8j_1$	0.0980(3)	0.0980(3)	0.2055(3)
Fe(4)	$8j_2$	0.3170(3)	0.3170(3)	0.2443(3)
Fe(5)	4e	0.000	0.000	0.6083(5)
Fe(6)	4c	0.000	0.500	0.000
C,B	4g	0.3721(7)	0.6279(7)	0.000

$B_{Ce} = 0.99(12)$ Å^2, $B_{Fe} = 0.71(2)$ Å^2, $B_{C,B} = 1.37(15)$ Å^2
$a,b = 8.7462(2)$ Å, $c = 11.8675(4)$ Å
$R_{nuclear} = 4.4\%$, $R_{profile} = 6.3\%$, $R_{expected} = 3.9\%$

The standard deviations of the lattice constants do not include errors $\Delta\lambda/\lambda$ from the neutron wavelength.

TABLE 3. Structural and magnetic parameters of $Ce_2Fe_{14}C_{0.95}B_{0.05}$ at 295 K (magnetic moments are fixed parallel to the c axis)

Atom	Position	Parameter			$\mu \parallel c$ (μ_B)
		x	y	z	
Ce(1)	4f	0.2612(10)	0.2612(10)	0.000	0.0
Ce(2)	4g	0.1422(10)	0.8578(10)	0.000	0.0
Fe(1)	$16k_1$	0.2243(4)	0.5653(4)	0.1213(3)	0.5(2)
Fe(2)	$16k_2$	0.0361(3)	0.3577(4)	0.1765(3)	1.2(2)
Fe(3)	$8j_1$	0.0979(4)	0.0979(4)	0.2052(3)	0.8(3)
Fe(4)	$8j_2$	0.3169(3)	0.3169(3)	0.2440(4)	1.9(2)
Fe(5)	4e	0.000	0.000	0.6079(5)	1.1(3)
Fe(6)	4c	0.000	0.500	0.000	1.9(2)
C,B	4g	0.3712(8)	0.6288(8)	0.000	0.0

$B_{Ce} = 0.79(14)$ Å^2, $B_{Fe} = 0.80(3)$ Å^2, $B_{C,B} = 1.81(19)$ Å^2
$a,b = 8.7611(2)$ Å, $c = 11.8918(5)$ Å
$R_{nuclear} = 4.3\%$, $R_{magnetic} = 5.4\%$, $R_{profile} = 6.7\%$, $R_{expected} = 3.6\%$

The standard deviations of the lattice constants do not include errors $\Delta\lambda/\lambda$ from the neutron wavelength.

TABLE 4. Structural and magnetic parameters of $Ce_2Fe_{14}C_{0.95}B_{0.05}$ at 12 K (magnetic moments are fixed parallel to the c axis)

Atom	Position	Parameter			$\mu \parallel c$ (μ_B)
		x	y	z	
Ce(1)	4f	0.2630(9)	0.2630(9)	0.000	−0.4(2)
Ce(2)	4g	0.1436(9)	0.8564(9)	0.000	−0.6(2)
Fe(1)	$16k_1$	0.2255(3)	0.5644(3)	0.1215(2)	1.4(2)
Fe(2)	$16k_2$	0.0357(3)	0.3578(4)	0.1752(2)	2.2(1)
Fe(3)	$8j_1$	0.0976(3)	0.0976(3)	0.2048(3)	2.1(2)
Fe(4)	$8j_2$	0.3173(3)	0.3173(3)	0.2445(3)	2.9(1)
Fe(5)	4e	0.000	0.000	0.6075(5)	1.2(3)
Fe(6)	4c	0.000	0.500	0.000	2.1(2)
C,B	4g	0.3723(7)	0.6277(7)	0.000	0.0

$B_{Ce} = 0.24(12)$ Å^2, $B_{Fe} = 0.61(3)$ Å^2, $B_{C,B} = 1.26(17)$ Å^2
$a,b = 8.7761(2)$ Å, $c = 11.8907(5)$ Å
$R_{nuclear} = 4.4\%$, $R_{magnetic} = 4.1\%$, $R_{profile} = 6.3\%$, $R_{expected} = 3.6\%$

The standard deviations of the lattice constants do not include errors $\Delta\lambda/\lambda$ from the neutron wavelength.

4. Discussion

Both compounds $R_2Fe_{14}C_{0.95}B_{0.05}$ ($R \equiv Ce$, Pr) crystallize in the same space group $P4_2/mnm$ as reported previously for $Nd_2Fe_{14}B$ [22]. The amount of 5% B instead of carbon is sufficient to stabilize the tetragonal structure and to avoid the formation of $R_2Fe_{17}C_x$ (Th_2Zn_{17} type). The lattice constants at room temperature determined by X-ray diffraction methods are $a = 8.7579(3)$ Å, $c = 11.8867(8)$ Å, for $R \equiv Ce$ and $a = 8.8138(5)$ Å, $c = 12.0541(15)$ Å, for $R \equiv Pr$.

The lattice constants for $Ce_2Fe_{14}C_{0.95}B_{0.05}$ exhibit a strong decrease at 423 K (Fig. 7), as determined by neutron diffraction measurements under identical experimental conditions. The reason for this is the Invar

TABLE 5. Magnetic moments of the iron atoms in $Ce_2Fe_{14}C_{0.95}B_{0.05}$ at 12 K with and without refinement of magnetic moments of the cerium atoms

	Values for the following Fe sites						$R_{nuclear}$	$R_{magnetic}$	$R_{profile}$
	$16k_1$	$16k_2$	$8j_1$	$8j_2$	4c	4e			
μ_{Fe} ($\mu_{Ce}\neq 0$)	1.4	2.2	2.1	2.9	1.2	2.1	4.4%	4.1%	6.3%
μ_{Fe} ($\mu_{Ce}=0$)	1.3	2.3	1.9	3.0	1.7	2.5	4.5%	4.5%	6.3%

The R values are given for comparison reasons.

TABLE 6. Structural parameters of $Pr_2Fe_{14}C_{0.95}B_{0.05}$ at 643 K

Atom	Position	Parameter		
		x	y	z
Pr(1)	4f	0.2577(9)	0.2577(9)	0.000
Pr(2)	4g	0.1408(10)	0.8592(10)	0.000
Fe(1)	$16k_1$	0.2241(4)	0.5661(3)	0.1217(2)
Fe(2)	$16k_2$	0.0366(3)	0.3584(4)	0.1786(3)
Fe(3)	$8j_1$	0.0985(4)	0.0985(4)	0.2096(3)
Fe(4)	$8j_2$	0.3173(3)	0.3173(3)	0.2447(4)
Fe(5)	4e	0.000	0.000	0.6083(5)
Fe(6)	4c	0.000	0.500	0.000
C,B	4g	0.3709(8)	0.6291(8)	0.000

$B_{Pr}=0.77(14)$ Å^2, $B_{Fe}=0.94(2)$ Å^2, $B_{C,B}=2.12(19)$ Å^2
$a,b=8.8260(3)$ Å, $c=12.0827(5)$ Å
$R_{nuclear}=5.0\%$, $R_{profile}=6.9\%$, $R_{expected}=3.8\%$

The standard deviations of the lattice constants do not include errors $\Delta\lambda/\lambda$ from the neutron wavelength.

TABLE 7. Structural and magnetic parameters of $Pr_2Fe_{14}C_{0.95}B_{0.05}$ at 295 K (magnetic moments are fixed parallel to the c axis)

Atom	Position	Parameter			$\mu\|c$ (μ_B)
		x	y	z	
Pr(1)	4f	0.2628(9)	0.2628(9)	0.000	1.5(2)
Pr(2)	4g	0.1428(8)	0.8572(8)	0.000	2.7(2)
Fe(1)	$16k_1$	0.2241(4)	0.5653(4)	0.1222(3)	1.9(1)
Fe(2)	$16k_2$	0.0358(3)	0.3588(4)	0.1769(3)	2.5(1)
Fe(3)	$8j_1$	0.0981(4)	0.0981(4)	0.2087(3)	2.0(2)
Fe(4)	$8j_2$	0.3171(3)	0.3171(3)	0.2448(4)	2.9(2)
Fe(5)	4e	0.000	0.000	0.6060(5)	2.0(3)
Fe(6)	4c	0.000	0.500	0.000	2.4(2)
C,B	4g	0.3735(9)	0.6265(9)	0.000	0.0

$B_{Pr}=0.52(14)$ Å^2, $B_{Fe}=0.87(3)$ Å^2, $B_{C,B}=1.73(19)$ Å^2
$a,b=8.8187(2)$ Å, $c=12.0626(5)$ Å
$R_{nuclear}=4.1\%$, $R_{magnetic}=5.4\%$, $R_{profile}=6.0\%$, $R_{expected}=3.3\%$

The standard deviations of the lattice constants do not include errors $\Delta\lambda/\lambda$ from the neutron wavelength.

anomaly. Neutron diffraction measurements at 423 K and at 643 K revealed no difference except the change in lattice constants and a slight change of the Ce(2) parameters. A pronounced change in the coordination sphere of the cerium atoms could not be observed;

TABLE 8. Structural and magnetic parameters of $Pr_2Fe_{14}C_{0.95}B_{0.05}$ at 23 K (magnetic moments are fixed parallel to the c axis)

Atom	Position	Parameter			$\mu\|c$ (μ_B)
		x	y	z	
Pr(1)	4f	0.2646(7)	0.2646(7)	0.000	2.7(1)
Pr(2)	4g	0.1418(6)	0.8582(6)	0.000	3.3(1)
Fe(1)	$16k_1$	0.2252(3)	0.5655(3)	0.1224(2)	2.4(1)
Fe(2)	$16k_2$	0.0356(3)	0.3593(3)	0.1772(2)	2.6(1)
Fe(3)	$8j_1$	0.0983(3)	0.0983(3)	0.2078(3)	2.5(1)
Fe(4)	$8j_2$	0.3174(2)	0.3174(2)	0.2455(3)	3.3(1)
Fe(5)	4e	0.000	0.000	0.6054(4)	2.1(2)
Fe(6)	4c	0.000	0.500	0.000	3.1(2)
C,B	4g	0.3743(6)	0.6257(6)	0.000	0.0

$B_{Pr}=0.61(11)$ Å^2, $B_{Fe}=0.62(2)$ Å^2, $B_{C,B}=0.70(13)$ Å^2
$a,b=8.8193(2)$ Å, $c=12.0566(4)$ Å
$R_{nuclear}=4.1\%$, $R_{magnetic}=4.9\%$, $R_{profile}=6.0\%$, $R_{expected}=3.2\%$

The standard deviations of the lattice constants do not include errors $\Delta\lambda/\lambda$ from the neutron wavelength.

therefore a change in the electron configuration is not assumed. A relation to the change in the specific heat capacity observed by means of DTA is assumed. The cerium atoms at 12 K have small magnetic moments due to a possible polarization-induced 5d moment or due to a not completely tetravalent electron configuration. At higher temperatures, *i.e.* 77 K ($Ce_2Fe_{14}B$ [23]) and room temperature (present work), these small magnetic moments disappear. The magnetic iron moments are 27.7(7) μ_B (formula unit)$^{-1}$ in comparison with 25.7 μ_B (formula unit)$^{-1}$ for $Ce_2Fe_{13.7}Mn_{0.3}C$ at 20 K determined by means of Mössbauer spectroscopy [24], with 30.6 μ_B (formula unit)$^{-1}$ for $Ce_2Fe_{14}B$ at 4.2 K determined by means of bulk magnetization [25] and with 36.3(5) μ_B (formula unit)$^{-1}$ for $Ce_2Fe_{14}B$ at 77 K determined by means of neutron diffraction [23].

For $Pr_2Fe_{14}C_{0.95}B_{0.05}$ the lattice constant a remains constant within the standard deviations with increasing temperature, from 23 K to 295 K, while c increases by $\Delta c=0.0065(6)$ Å, as determined by neutron diffraction measurements under identical experimental conditions. The magnetic iron moments are 36.8(4) μ_B (formula unit)$^{-1}$ at 23 K, while all magnetic moments are 42.8(5) μ_B (formula unit)$^{-1}$ compared with

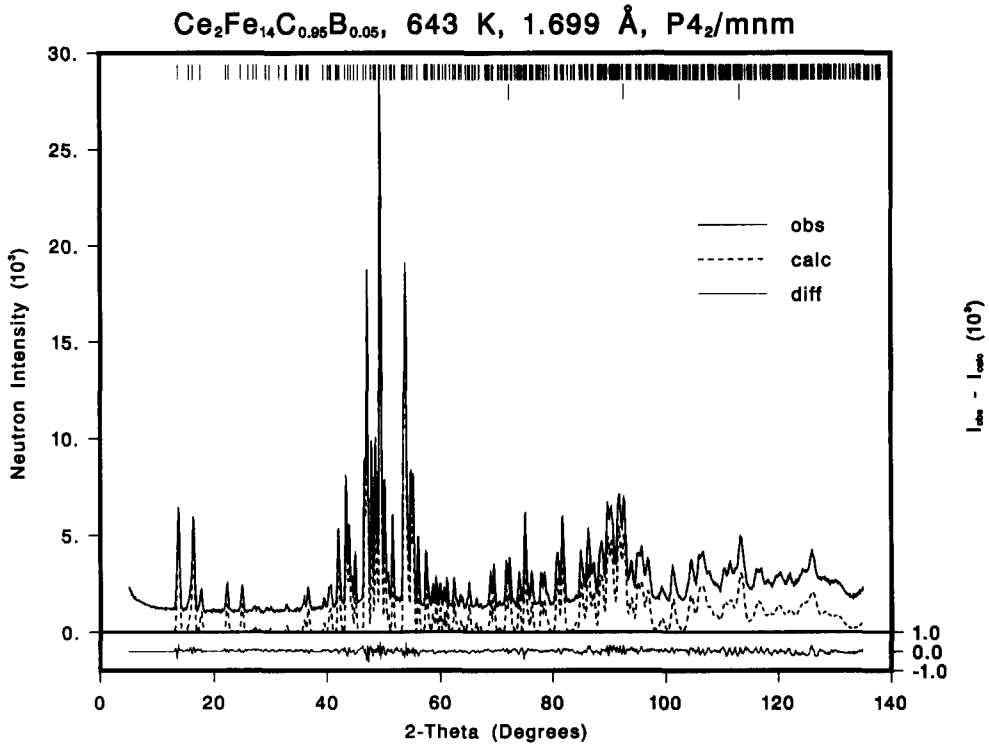

Fig. 3. Observed and calculated neutron diffraction patterns of paramagnetic $Ce_2Fe_{14}C_{0.95}B_{0.05}$ at 643 K. The lines at the top indicate the positions of the following reflections: upper row, $Ce_2Fe_{14}C_{0.95}B_{0.05}$; lower row, α-Fe.

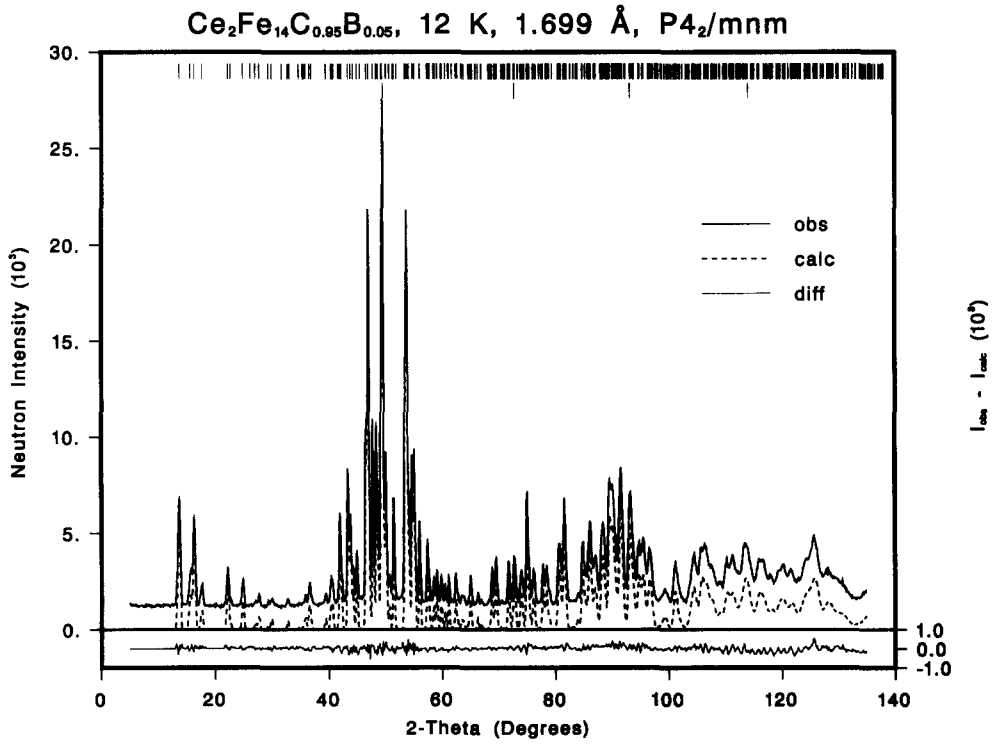

Fig. 4. Observed and calculated neutron diffraction patterns of ferromagnetic $Ce_2Fe_{14}C_{0.95}B_{0.05}$ at 12 K. The lines at the top indicate the positions of the following reflections: upper row, $Ce_2Fe_{14}C_{0.95}B_{0.05}$; lower row, α-Fe.

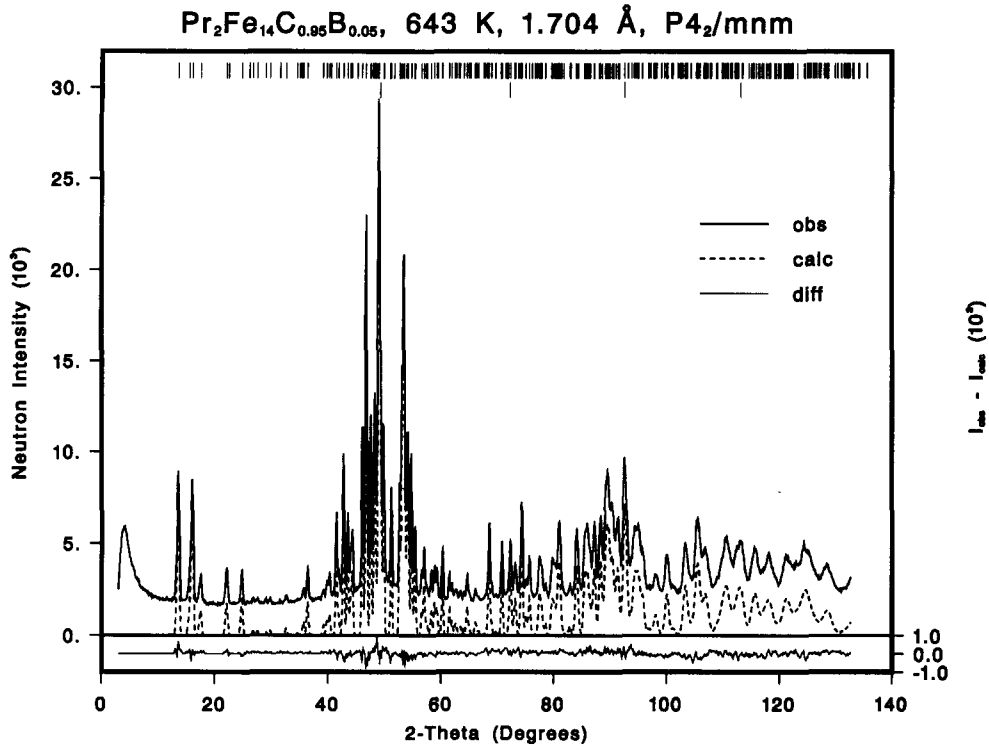

Fig. 5. Observed and calculated neutron diffraction patterns of paramagnetic $Pr_2Fe_{14}C_{0.95}B_{0.05}$ at 643 K. The lines at the top indicate the positions of the following reflections: upper row, $Pr_2Fe_{14}C_{0.95}B_{0.05}$; lower row, α-Fe.

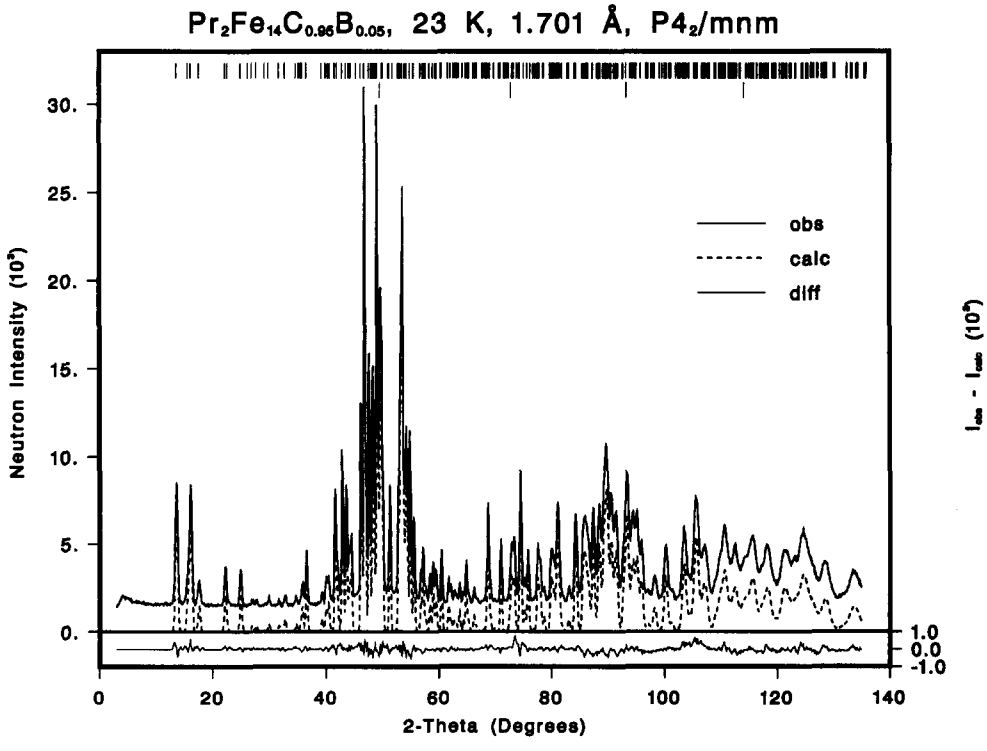

Fig. 6. Observed and calculated neutron diffraction patterns of ferromagnetic $Pr_2Fe_{14}C_{0.95}B_{0.05}$ at 23 K. The lines at the top indicate the positions of the following reflections: upper row, $Pr_2Fe_{14}C_{0.95}B_{0.05}$; lower row, α-Fe.

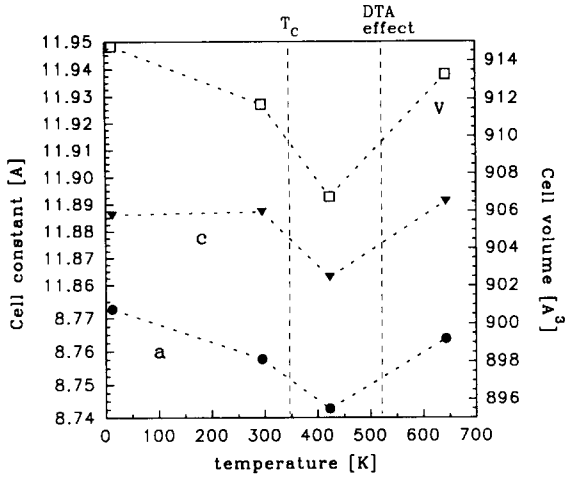

Fig. 7. Observed cell constants and volume of $Ce_2Fe_{14}C_{0.95}B_{0.05}$ at different temperatures as determined by neutron diffraction measurements under identical experimental conditions. The values are corrected with respect to the room temperature X-ray data. – – –, guides for the eye.

36.3 μ_B (formula unit)$^{-1}$ for $Pr_2Fe_{14}B$ at 4.2 K determined by means of bulk magnetization [25].

5. Conclusions

The neutron diffraction data obtained for $R_2Fe_{14}C_{0.95}B_{0.05}$ ($R \equiv Ce$, Pr) in the course of the present investigation confirm that the compounds have the tetragonal $Nd_2Fe_{14}B$ structure. The small boron content was sufficient to avoid the formation of a second intermetallic phase. The magnetic moments of the iron and the praseodymium atoms order ferromagnetically below the Curie temperature with moments oriented along the *c* direction. For the cerium atoms at 12 K small magnetic moments could be refined. A strong decrease in volume at 423 K and a change in specific heat capacity at 515 K were measured for $Ce_2Fe_{14}C_{0.95}B_{0.05}$.

Acknowledgments

We wish to thank the workshop group of LNS (especially Mr. M. Koch) and the PSI reactor division for support and Professor P. Wachter for his interest. This work has been supported by the Swiss National Science Foundation.

References

1 M. Sagawa, S. Fujimura, M. Togawa and Y. Matsuura, *J. Appl. Phys., 55* (1984) 2083.
2 K. H. J. Buschow, in E. P. Wohlfarth and K. H. J. Buschow (eds.), *Ferromagnetic Materials,* Vol. 4, North-Holland, Amsterdam, 1988, p. 1.
3 E. P. Marusin, O. I. Bodak, A. O. Tsokol and V. S. Fundamenskii, *Sov. Phys. Crystallogr., 30* (1985) 338.
4 C. Abache and H. Oesterreicher, *J. Appl. Phys., 57* (1985) 4112.
5 A. T. Pedziwiatr, W. E. Wallace and E. Burzo, *J. Magn. Magn. Mater., 59* (1986) L179.
6 N. C. Liu and H. H. Stadelmaier, *Mater. Lett., 4* (1986) 377.
7 M. Gueramian, A. Benzinge, K. Yvon and J. Müller, *Solid State Commun., 64* (1987) 639.
8 C. J. M. Denissen, B. D. de Mooij and K. H. J. Buschow, *J. Less-Common Met., 142* (1988) 195.
9 D. B. de Mooij and K. H. J. Buschow, *J. Less-Common Met., 142* (1988) 349.
10 Ch. Hellwig, K. Girgis, J. Schefer, K. H. J. Buschow and P. Fischer, *J. Less-Common Met., 169* (1991) 147.
11 Ch. Hellwig, K. Girgis, R. Coehoorn, J. Schefer, K. H. J. Buschow and P. Fischer, *J. Alloys Comp., 184* (1992) 161.
12 Ch. Hellwig, K. Girgis, J. Schefer, K. H. J. Buschow and P. Fischer, *J. Alloys Comp., 184* (1992) 175.
13 Ch. Hellwig, K. Girgis, J. Schefer, K. H. J. Buschow and P. Fischer, *J. Less-Common Met., 163* (1990) 361.
14 M. Yethiraj, W. B. Yelon and K. H. J. Buschow, *J. Magn. Magn. Mater., 97* (1991) 45.
15 J. Schefer, P. Fischer, H. Heer, A. Isacson, M. Koch and R. Thut, *Nucl. Instrum. Methods A, 288* (1990) 477.
16 V. F. Sears, *Methods Exp. Phys., A, 23* (1986) 521.
17 L. Koester, H. Rauch and E. Seymann, *At. Data Nucl. Data Tables, 49* (1991) 65.
18 A. J. Freeman and J. P. Desclaux, *J. Magn. Magn. Mater., 12* (1979) 11.
19 R. M. Moon, *Int. J. Magn., 1* (1971) 219.
20 H. M. Rietveld, *J. Appl. Crystallogr., 2* (1969) 65.
21 A. W. Hewat, *Rep. AERE-R7350,* 1973 (Atomic Energy Research Establishment, Harwell).
22 J. F. Herbst and W. B. Yelon, *J. Appl. Phys., 60* (1986) 4224.
23 J. F. Herbst and W. B. Yelon, *J. Magn. Magn. Mater., 54–57* (1986) 570.
24 T. H. Jacobs, C. J. M. Denissen and K. H. J. Buschow, *J. Less-Common Met., 153* (1989) L5.
25 E. B. Boltich, E. Oswald, M. Q. Huang, S. Hirosawa, W. E. Wallace and E. Burzo, *J. Appl. Phys., 57* (1985) 4106.